Intelligent Power System Frequency Regulations Concerning the Integration of Wind Power Units

H. Bevrani, F. Daneshfar, and R.P. Daneshmand

As the use of wind power turbines increases worldwide, there is a rising interest on their impacts on power system operation and control. Frequency regulation in interconnected networks is one of the main challenges posed by wind turbines in modern power systems. The wind power fluctuation negatively contributes to the power imbalance and frequency deviation. Significant interconnection frequency deviations can cause under/over frequency relaying and disconnect some loads and generations. Under unfavorable conditions, this may result in a cascading failure and system collapse.

This chapter presents an overview of the key issues on frequency regulation concerning the integration of wind power units into the power systems. Following a brief survey on the recent developments, the impact of power fluctuation produced by wind units on system frequency performance is presented. An updated frequency response model is introduced, and the inertia contribution of wind turbine in the overall system inertia is properly considered. The need for the revising of frequency performance standards is emphasized, and an intelligent agent based load frequency control (LFC), using multi-agent reinforcement learning (MARL) is proposed. Finally, nonlinear time-domain simulations on a 39-bus test power system are used to demonstrate the capability of the proposed control structure, and to analyze the system frequency performance in the presence of high wind power penetration and associated issues.

1 Introduction

The increasing need for electrical energy in the twenty-first century, as well as limited fossil fuel reserves, very high transportation and fuel cost and the increasing concerns with environmental issues for the reduction of carbon dioxide (CO2) and

H. Bevrani · F. Daneshfar · R.P. Daneshmand
Department of Electrical and Computer Engineering, University of Kurdistan, Sanandaj, PO Box 416, Iran

L. Wang et al. (Eds): *Wind Power Systems*, Green Energy and Technology, pp. 407–437.
springerlink.com

other greenhouse gasses [40], causes fast development in the area of renewable energy sources (RESs).

RESs are derived from natural sources such as the sun, wind, hydro-power, biomass, geothermal, oceans, and fuel cells that replenished themselves over a relatively short period of time. The most kind of the RES used is wind energy which is clean and available in nature. The wind turbine generators have attracted a lot of attention. Nowadays, the electric power industry has become more complicated than ever. It is necessary to interconnect more distributed generations in power systems because of environmental concerns. Primary concern includes global environmental and energy depletion issues. In addition to the energy security and deregulation matters which affect the so-called business chances. Therefore, the distributed generations, especially wind power generations, attract attentions in many countries.

Since, the primary energy source (wind) cannot be stored and is uncontrollable, the controllability and availability of wind power significantly differs from conventional power generation. In most power systems the output power of wind turbine generators varies with wind speed fluctuation, this fluctuation results into frequency variation [15, 19, 30]. Some reports are recently addressed the power system frequency control issue, in the presence of wind turbines [10, 13, 23, 25, 26, 27, 29, 32, 33, 37]. In this direction, the load-frequency control (LFC) is one of important control problems in concerning the integration of wind power turbine in a multi-area power system [2, 8, 18, 20, 21, 31].

Using conventional linear control methodologies for the LFC design in a modern power system is not more efficient, because they are only suitable for a specific operating point in a traditional structure. If the dynamic/structure of system varies; they may not perform as expected. Most of conventional control strategies provide model based controllers that are highly dependent to the specific models, and are not useable for large-scale power systems concerning the integration of RES units with nonlinearities, undefined parameters and uncertain models. If the dimensions of the power system increase, then these control design may become more different as the number of the state variables also increases, significantly.

Therefore, design of intelligent controllers that are more adaptive and flexible than conventional controllers is become an appealing approach. Intelligent control has been already used for the frequency regulation issue in the power systems [14, 24, 44]; however there are just few reports on the frequency control design in the presence of RES units [11].

One of the adaptive and nonlinear intelligent control techniques that can be effectively applicable in the frequency control design is reinforcement learning (RL). Some efforts are addressed in [3, 4, 5, 7, 16, 17]. RL based controllers learn and are adjusted to keep the area control error small enough in each sampling time of a LFC cycle. Since, these controllers are based on learning methods; they are independent of environment conditions and can learn a wide range of operating conditions. The RL based frequency control design is a model-free design and can easily scalable for large scale systems and suitable for frequency variation caused by wind turbine fluctuation.

In the continuation of the authors' recent works [9, 11], the present chapter addresses the LFC design using an agent based reinforcement learning for a large interconnected power system concerning the integration of wind power units. In this chapter, a multi-agent RL based control structure is proposed. Each control area includes an agent that communicates with each other to control the frequency among whole interconnected system. Each agent (controller agent) provides an appropriate control action according to the area control error (*ACE)* signal, using reinforcement learning. In a multi-area power system, the learning process is considered as a multi-agent RL process and agents of all areas learn together (not individually).

The above technique has been applied to the LFC problem in a network with the same topology as IEEE 10 generators 39-bus test system integrated with wind power units, as a case study. The rest of chapter is organized as follows: In Section 2.2, the impact of wind power generation on power system frequency and the structure of a network which the above architecture is implemented for, are discussed. A generalized frequency response model is introduced, and the need for revising of frequency performance standards is emphasized.

In Section 2.3, a brief introduction to single-agent and multi-agent based RL is presented. Section 2.4 and 2.5 address the proposed intelligent frequency control technique using agent based RL. It is explained that how the designed controllers for the test system can work. Simulation results are provided in Section 2.6 and the chapter is concluded in Section 2.7.

2 Impacts of Wind Power Generation on the Power System Frequency and Frequency Regulation

Dynamic behavior of a power system in the presence of wind power generation systems might be different from conventional power plants. The power outputs of such sources are dependent on weather conditions, seasons, and geographical location. When wind power is a part of the power system, additional imbalance is created when the actual wind power deviates from its forecast due to wind velocity variations. So, scheduling conventional generator units to follow load (based on the forecasts) may also be affected by wind power output [11]. Furthermore, the effect of wind farms on the dynamic behavior of power system may cause a different system frequency response to a disturbance event (such as load disturbance).

Since, the system inertia determines the sensitivity of overall system frequency; it plays an important role in this consideration [11]. The lower system inertia, lead to faster changes in the system frequency following a load generation variation. The addition of synchronous generation to a power system intrinsically increases the system inertial response. This intrinsic increase does not necessarily with the addition of wind turbine generators (WTGs) due to their differing electromechanical characteristic [28]. So, the impact of wind farms on power system inertia is a key factor in investigating the power system frequency behavior in the presence of high penetration wind power generation.

Depending on the technology is used in installed wind turbine generators; proportion of wind power generation on system inertia could be different. Thus, in order to analyze the impact of WTGs on system inertia (and consequently on system frequency) it is important to consider the wind generation technologies.

2.1 Wind Generation Technologies

Generally, there are two basic categories of wind turbine generators; fixed speed and variable speed WTGs. Here, a brief description is given for these wind turbine technologies.

Fixed Speed WTGs

Fixed Speed WTGs generally use squirrel-cage induction generators. Stator winding of the generator is directly connected to the grid. The rotor of the turbine blades is coupled to the rotor of the generator through a gearbox. So, the turbine could utilize the kinetic energy stored in the turbine blades and contributes to the system frequency stability by providing spinning inertia [41].

When the system frequency deviates from its nominal value, the relationship between the system frequency and electromagnetic torque of induction generator will determine the inertial response. Strong coupling between the squirrel-cage induction generator stator and power system and low nominal slip (about one to two percent [34]) of them cause any deviation in the system speed lead to a change in rotational speed. Such linking between rotor speed and system frequency gives rise to an inertial response from the fixed speed WTGs during a system frequency falling.

Generally, the fixed speed turbines have a simple construction. However, as they cannot track wind speed fluctuations the energy capture is not as efficient as in variable speed systems. As a wind rotor presents maximum power coefficient at its design tip speed ratio (TSR), for constant speed operation this maximum power coefficient can be reached to its designed wind speed [28, 36, 41]. Fig. 1 shows a general configuration for a fixed speed wind turbine generator.

Variable Speed WTGs

Variable speed WTGs could be equipped with either synchronous generators or doubly-fed induction generators (DFIG).

In the case of synchronous generators, the wind turbine is allowed to spin at whatever speed that is needed to reached maximum power. So, the electrical output frequency would vary due to instantaneous variation in the wind velocity. As a result, the generator cannot be directly connected to the grid due to its poor power quality. In the variable speed application these generators are decoupled from the grid through the use of a back-to -back *ac/dc/ac* converter attached to the stator of the synchronous generator.

First, the variable frequency *ac* output of generator is rectified into *dc* using high power switching transistors; then, the *dc* converts back to *ac* at grid

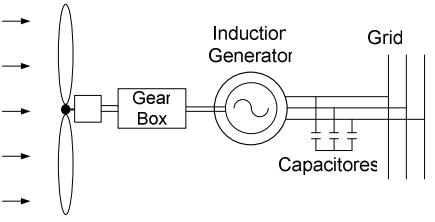

Fig. 1. Fixed speed wind turbine generator

frequency through an inverter before feeding to the grid. This design causes the stator be isolated from power system and do not touch frequency variations. Therefore, during a frequency event wind turbine generator has no inertial response and its power output does not change.

Another and more common variable speed wind turbine technology is the DFIG which uses wound-rotor induction machines. In this type, stator winding is directly connected to the grid. However, the rotor winding is connected to the power system by employing a back-to-back *ac/dc/ac* converter which varies the electrical frequency as acceptable by the grid. Thus, the electrical frequency will be different from the mechanical frequency which allows for variable speed application. This converter allows for the control of active and reactive power using constant power factor or constant voltage [36, 41].

When a frequency event occurs, the inertial response provided by the DFIG depends on the relationship between electromagnetic torque of the machine and power system frequency. This relationship depends on the control structure used in the converter and their parameters [35].

Variable speed WTGs present higher energy capturing, lower mechanical stress, more constant output power, and reduced noise compared with fixed speed machines [1]. This type of wind power technology is more common than the other. From this type, DFIGs are more popular and comprise the predominant portion of the installed wind energy. Fig. 2 shows simple configurations for the variable speed wind turbine generators.

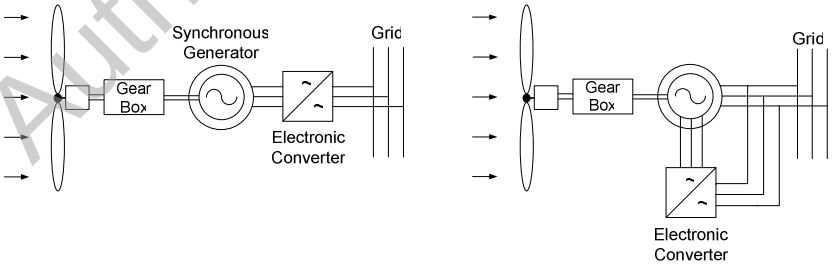

(a) (b)

Fig. 2. Variable speed wind turbine generators; (a) with synchronous generator, (b) with doubly fed induction generator (DFIG)

2.2. System Response Analysis

To investigate the impact of wind power generation on the power system (particularly on system frequency), a simulation study is provided in the Simpower environment of MATLAB software. Here, the power system response for a test system is shown under normal and alert conditions in the presence of WTGs.

Test System

As mentioned, the wind power generation could affect the dynamic behavior of the power system. The frequency response characteristic of a power system with a high penetration of wind power may be different from that of the conventional system [11]. This section provides a simulation study on the impacts of wind power unit, particularly DFIG wind power generation on the power system frequency. For this purpose, a network with the same topology as the well-known IEEE 10 generators 39-bus test system is considered as a case study.

This test system is widely used as a standard system for testing of new power system analysis and control synthesis methodologies. A single-line diagram of the system is given in Fig. 3. It represents a greatly reduced model of the power system in New England. It can be used to study both static and dynamic problems in the power system. This system has 10 generators, 19 loads, 34 transmission lines, and 12 transformers. The simulation parameters for the generators, loads, lines, and transformers of the test system are given in Appendix.

The 39 buses system is organized into 3 areas. Total system installed capacity are 841.2 MW of conventional generation and 45.34 MW of wind power generation. There are 198.96 MW of conventional generation, 22.67 MW of wind power generation and 265.25 MW load in Area 1. In Area 2, there are 232.83 MW of conventional generation, and 232.83 MW load. In Area 3, there are 160.05 MW of conventional generation, 22.67 MW of wind power generation and 124.78 MW of load.

All power plants in the power system are equipped with speed governor and power system stabilizer (PSS). However, only one generator in each area is responsible for the LFC task using a well-tuned proportional integral (PI) controller; G1 in Area 1, G9 in Area 2, and G4 in Area 3.

For the sake of simulation, random variations of wind velocity have been considered. Dynamics of WTGs including the pitch angle control of the blades are also considered. The start up and rated wind velocity for the wind farms are specified as about 8.16 (m/s) and 14 (m/s), respectively. Furthermore, the pitch angle controls for the wind blades are activated only beyond the rated wind velocity. The pitch angles are fixed to zero degree at the lower wind velocity below the rated one.

Impact of WTGs on System Frequency in a Normal Operating Condition

When wind power plants are introduced into the power system, an imbalance is created when the actual wind output deviates from its forecast [11]. This power imbalance may lead to frequency deviations from nominal value (60 Hz in the present example). Fig. 4 illustrates the frequency deviation due to wind power fluctuations.

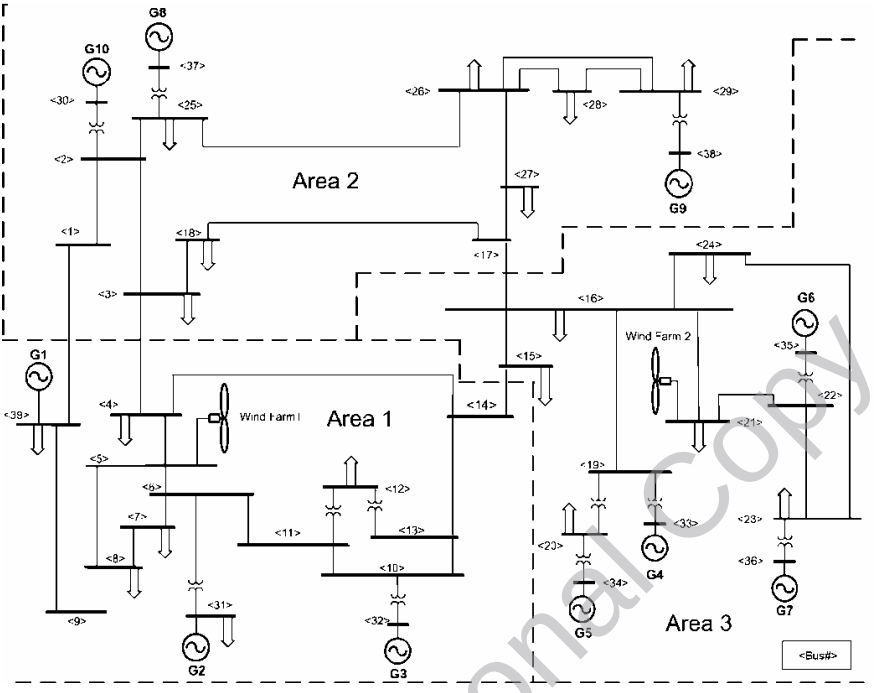

Fig. 3. Single-line diagram of 39-bus test system

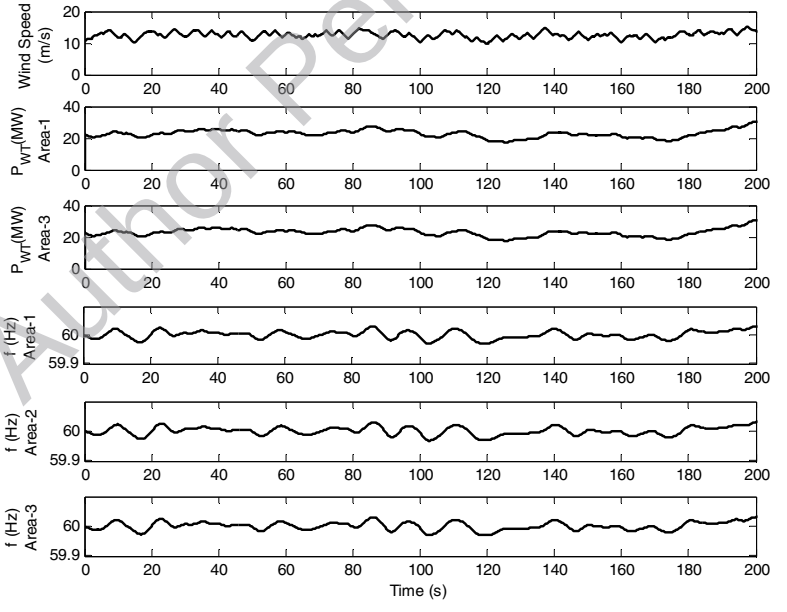

Fig. 4. System response to wind power fluctuations

From the power quality point of view, frequency deviations should be limited in a specified standard band. As shown in the simulation results, in the presence of wind power generation, the frequency regulation performance is significantly decreased.

Simulation results show that the generator units equipped with conventional PI controllers (G1, G9 and G4) are unable to provide a desirable frequency regulation following fluctuation caused by wind power variations.

Impacts of WTGs on the System Frequency under Load Disturbance Condition

Beside the normal condition, impact of high penetration wind power generation on system frequency at abnormal condition is also noticeable. As mentioned, adding of wind generators to a power system leads to increase in total system inertia. The most pronounce effect of high values of inertia is to reduce the initial rate of frequency decline, and to delay and reduce in the maximum deviation [6].

To investigate above issue, system response following a step load disturbance is investigated. A step load increase is considered at 10 s in each area as follows. 3.8 percent of area load at bus 8 in Area 1, 4.3 percent of area load at bus 3 in Area 2, and 6.4 percent of area load at bus 16 in Area 3 have been changed. System response is shown in Fig. 5. For having a clear comparison, a zoomed view of Fig. 5 around 10s is redrawn in Fig. 6.

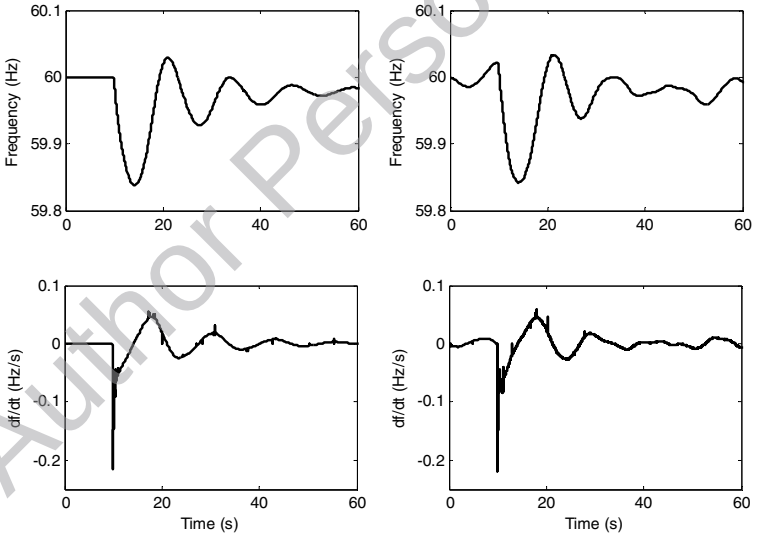

(a) (b)

Fig. 5. Overall system frequency and rate of frequency change to a simultaneous step load changes in three areas; (a) without WTGs, (b) with WTGs

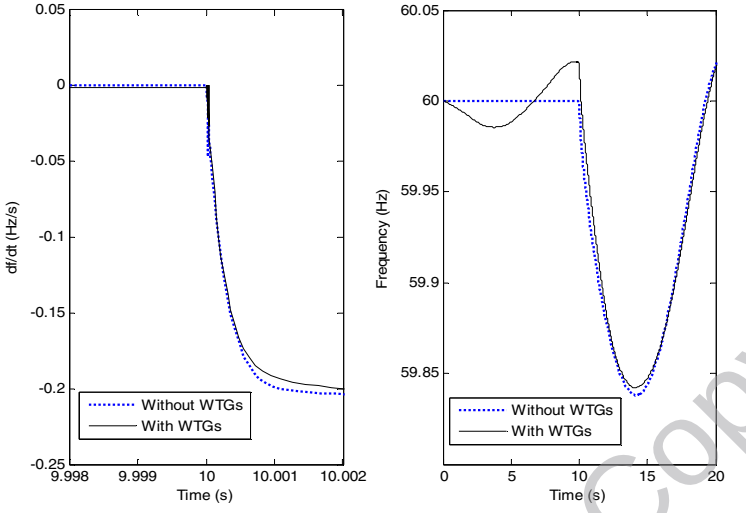

(a) (b)

Fig. 6. Frequency deviation following step load disturbances at 10 sec; (a) rate of frequency change, (b) system frequency

As shown in Fig. 6a, the initial rate of frequency change following a load disturbance, has reduced in the presence of WTGs; because the wind power penetration in the power system can increase the overall system inertia [11]. However, as DFIGs provide small inertial response, this reduction is not noticeable.

Maximum frequency deviation range following a step load disturbance is shown in Fig. 6. It could be seen that in the presence of WTGs, the frequency drop has reduced. It is justifiable by considering the larger inertia due to the addition of large wind farms to the system. The higher inertia value results in a lower drop in frequency. Since the response is slower for the higher inertia, the governor has more time to response and therefore limits the maximum frequency deviation to smaller value [6].

The Impact of High Penetration Wind Generation on the Required LFC Reserve

When WTGs are introduced to the power system, as they generate a part of power system loads, much portion of conventional nominal power can be available for using in supplementary control. However, as the variable wind farms power output may or may not be available during peak demand and abnormal periods, due to unpredictable nature of wind; it might be that these resources cannot contribute to the overall system frequency regulation and reliability. On the other hand, the additional power variation from WTGs results in frequency deviation. It seems that for a large wind power penetration, this deviation will be so larger and as a result, the conventional LFC reserve may be insufficient to maintain frequency within the bounds for service quality.

It was found that wind power, does not impose major extra variations on the system until a substantial penetration is reached [11]. Large geographical spreading of wind power will reduce variability, increases predictability, and decrease the occasions with near zero or peak output [22]. It is investigated in [11] that the power fluctuation from geographically dispersed wind farms will be uncorrelated with each other, hence smoothing the sum power and not imposing any significant requirement for additional frequency regulation reserve, and required extra balancing is small.

The fluctuation of the aggregated wind power output in a short term (e.g., tens of seconds) for a larger number of wind turbines are much smoothed. It is investigated that the wind turbines aggregation has positive effects on the regulation requirement. Relative regulation requirement decreases whenever larger aggregations are considered [22].

To show the impact of large aggregation of wind turbines on wind power outputs smoothing and required supplementary reserve, a simulation study was applied on the test case system with considering high penetration wind power in Area 1 and Area 3. The effect of wind power on frequency, following the step load disturbance can be investigated in Fig. 7. To show the impact of wind farm size on power smoothing two conditions are considered: occurrence of the load disturbance in with considering average wind power output (neglecting wind power fluctuations), and with actual wind farms output.

It can be also seen in Fig. 7, that because of smoothing effect on wind power output fluctuations due to large penetration of wind farms, wind power fluctuations does not impose too much variations on the response of generators equipped with LFC, respect to the considering of average wind power output.

2.3 Generalized Area Frequency Response Model

To analyze the additional variation caused by WTGs, the total effect is important, and every change in wind power output does not need to be matched one for one by a change in another generating unit moving in the opposite direction. Instantaneous fluctuations in load and WTG power output might amplify each other, be completely unrelated to each other, or they may cancel each other out [11]. However, the slow WTG power fluctuation dynamics and total average power variation negatively contribute to the power imbalance and frequency deviation, which should be taken into account in the well-known LFC control scheme. This power fluctuation must be included in the conventional LFC structure.

A generalized LFC model in the presence of WTGs is shown in Fig. 8. Here, to cover the variety of generation types in the control area, different values for turbine-governor parameters and the generator regulation parameters are considered. Fig. 8 shows the block diagram of typical control area with n generator units. The shown blocks and parameters are defined as follows: Δf is frequency deviation, ΔP_m is mechanical power, T_{ij} is synchronizing coefficient, ΔP_c is supplementary control action, ΔP_L is load disturbance, H_{Sys} is equivalent inertia

constant, D_{Sys} is equivalent damping coefficient, B is frequency bias, R_i is drooping characteristic, ΔP_P is primary control, α_i is participation factors, ΔP_{WTG} is WTG power fluctuation, $K(s)$ is LFC controller, and $M_i(s)$ is governor-turbine model.

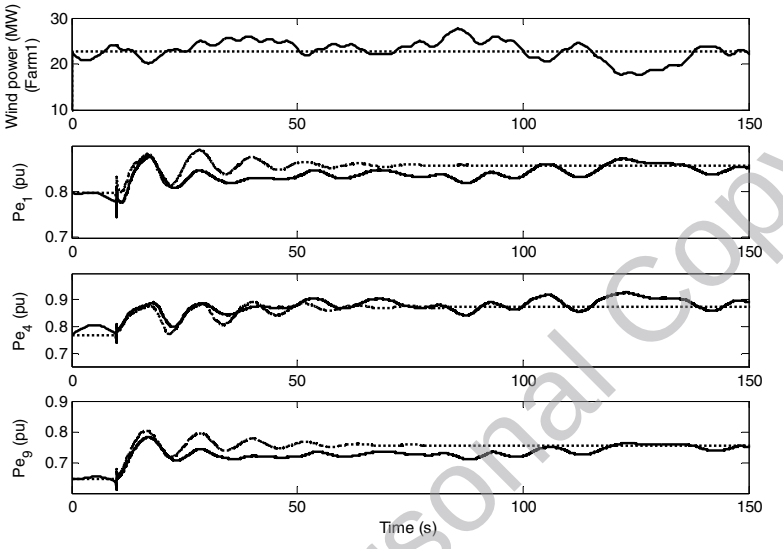

Fig. 7. Impact of wind power fluctuation on required supplementary LFC reserve; actual wind power (solid), average wind power (dotted)

Following a load disturbance within the control area, the frequency of the area experiences a transient change and the feedback mechanism generates appropriate rise or lower signal to the participating generator units according to their participation factors α_i to make generation follow the load. In the steady state, the generation is matched with the load, driving the tie-line power and frequency deviations to zero. As there are many conventional generators in each area, the control signal has to be distributed among them in proportion to their participation.

As shown in Fig. 8, the frequency performance of a control area is represented approximately by a lumped load generation model using equivalent frequency, inertia and damping factors [9]. Because of range of use and specific dynamic characteristics such as a considerable amount of kinetic energy, the wind units are more important than the other renewable energy resources. The equivalent system inertia can be defined as:

$$H_{sys} = H_C + H_W = \sum_{i=1}^{N1} H_{Ci} + \sum_{i=1}^{N2} H_{Wi} \tag{1}$$

The H_C and H_W are the total inertia constants due to conventional and wind turbine generators, respectively. The inertia constant for wind power is time dependant. The typical inertia constant for the wind turbines is about two to six seconds [11].

In Fig. 8, the filtered total effect of power fluctuation ΔP_{WTG} is considered. For a large WTGs penetration, the resulting *ACE* signal must reflect the total WTGs power generation changes which is usually smoothed compared to variations from the individual wind turbine units.

$$ACE = B\Delta f + \sum (P_{Con,act} - P_{Con,sched}) + \sum (P_{WTG,act} - P_{WTG,estim}) \tag{2}$$

where $P_{Con,act}$, $P_{Con,sched}$, $P_{WTG,act}$, and $P_{WTG,estim}$ are actual conventional power, scheduled conventional power, actual WTGs power, and estimated WTGs power, respectively.

In typical LFC implementations, the system frequency gradient and *ACE* signal must be filtered to remove noise effects before use. The *ACE* signal then is often applied to a proportional integral (PI) control block [9, 10]. Control dead band and ramping rate are different for various systems [11]. The control can send higher/lower pulses to generating plants if its *ACE* signal exceeds a standard limits.

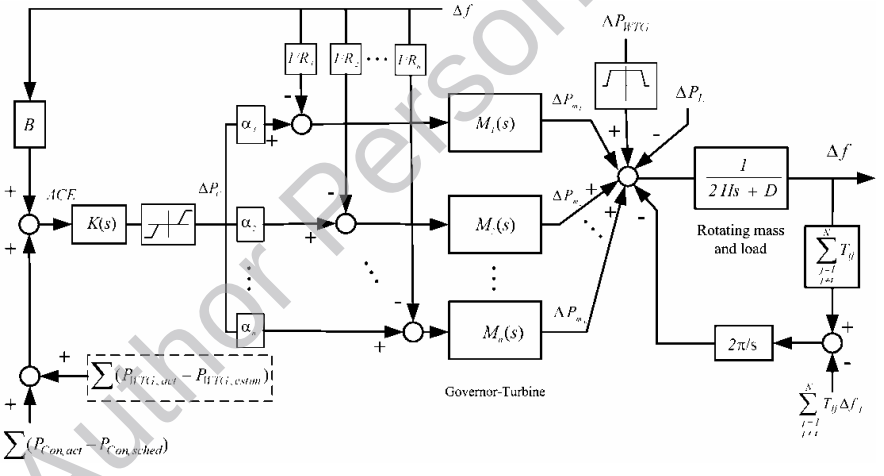

Fig. 8. LFC model with considering WTG power fluctuation

2.4 The Need for Revising of Frequency Performance Standards

Power system frequency control is an issue that may evolve into new guidelines. The existing frequency operating standards need to change to allow for the introduction of renewable power generation, and allow for modern distributed generator technologies.

It is investigated that the slow component of renewable power fluctuation negatively affects the performance standards such as policy P1 of UCTE (Union for the Coordination of Transmission of Electricity) performance standard, or the control performance standards CPS1 and CPS2 introduced by NERC (North American Electric Reliability Council) [11].

The standards redesign must be done in both normal and abnormal conditions, and should take account of operational experience on the initial frequency control schemes and again used measurement signals including tie-line power, frequency, and rate of frequency change settings. The new set of frequency performance standards are under development in many countries. The new standards introduce the update high and low trigger, abnormal, and relay limits applied on the interconnection frequency excursions.

The revised standards may bring an element of a more centralized frequency control through a better coordination among control areas, delegating more authority to the control areas performing frequency monitoring functions, and perhaps creating distributed or inter-area control centers to decentralized frequency control through the creation of corresponding ancillary service markets.

As mentioned, the rate of frequency change (df / dt) following a disturbance is proportional to the power imbalance, and it also depends on the equivalent system inertia [11]. Since large wind farms can considerably increase the overall system inertia, the df / dt will be significantly changed. From an operational point of view, a larger variable renewable power in the power system causes a smaller frequency rate change following a sudden loss of generation or load disturbance. This issue is important for those networks that use the protective df / dt relays to re-evaluate their tuning strategies.

The performance standards revision has already commenced in many countries [11]. In Australia, the Australian Electricity Market Commission (AEMC) is proposing revised technical rules for generator connection, including wind generators. As well as meeting technical standards, generators are required to provide information on energy production via the system operator's SCADA system. National Electricity Market Management Company (NEMMCO) sets out functional requirement for an Australian Wind Energy Forecasting System (AWEFS) for wind farms in market regions. In the USA, NERC is working to revise the conventional control performance standards. The existing market rules and priority rules for the transport of RES electricity is also under re-examination by UCTE in Europe.

3 A Background on Agent Based RL

The present section presents a brief background on the single-agent and multi-agent RL (MARL) [38]. First, the single-agent RL is defined and its solution is described. Then, the multi-agent task is defined. The discussion is restricted to finite state and action spaces, as the major part of MARL results are given for finite spaces [12].

3.1 Single-Agent RL

Reinforcement learning (RL) is learning what to do, how to map situations to actions, so as to maximize a numerical reward signal [16]. In fact the learner will discover which action should be taken by interacting with the system and trying the different actions which may lead to the highest reward. The RL will evaluate the actions taken and gives the learner a feedback of how good the action taken was and whether it should repeat this action in the same situation or not. In another word, the RL methods learn to solve a problem by interacting with a system. The learner is called the agent and the system it interacts with, is known as the environment. During the learning process, the agent interacts with the environment and takes an action a_t from a set of actions, at time t. These actions will affect the system and will take it to a new state x_{t+1}. Therefore, the agent is provided with the corresponding reward signal (r_{t+1}). This agent-environment interaction is repeated until the desired goal is achieved. In this text what is meant by the state is the required information for making a decision, therefore what we would like, ideally, is a state signal that summarizes past perceptions in a way that all relevant information is retained. A state signal that succeeds in retaining all relevant information is said to be Markov, or to have the Markov property [16] and a reinforcement learning task that satisfies this property is called a finite Markov Decision Process (MDP). If an environment has the Markov property, then its dynamics enable us to predict the next state and expected next reward given the current state and action.

In the present work, it is assumed that the environment has the Markov property; therefore a MDP problem is solved. In each MDP the objective is to maximize sum of returned rewards over time, then the expected sum of discounted rewards defined by the following equation:

$$R = \sum_{k=0}^{\infty} \gamma^k r_{t+1} \tag{3}$$

where $0 < \gamma < 1$ is a discount factor, which gives the most importance to the recent rewards.

Another term is value function that is defined as the expected return or reward (E) when starting at state x_t while following policy $\pi(x, a)$ (see Eq. 4). Policy is the way the agent maps the states to the actions [16].

$$V^{\pi}(x) = E_{\pi}\left\{\sum_{k=0}^{\infty} \gamma^k r_{t+k+1} | x_t = x\right\} \tag{4}$$

The optimal policy is one that maximizes the value function. Therefore, once the optimal state value is derived, the optimal policy can be found as follows:

$$V^*(x) = \max_{\pi} V^{\pi}(x) \ , \forall x \ \in X \tag{5}$$

In most RL methods, instead of calculating the state value, another term known as the action value is calculated (6), which is defined as the expected discounted reward while starting at state x_t and taking action a_t.

$$Q^{\pi}(x,a) = E_{\pi}\left\{\sum_{k=0}^{\infty}\gamma^{k} r_{t+k+1} | x_t = x, a_t = a\right\} \tag{6}$$

Bellman's equation [16], as shown below, is used to find the optimal action value. In general, an optimal policy is one that maximizes the Q-function defined in the following relation:

$$Q^{*}(x,a) = \max_{\pi} E_{\pi}\left\{r_{t+1} + \gamma \max_{\acute{a}} Q^{*}(x_{t+1}, \acute{a}) \mid x_t = x, a_t = a\right\} \tag{7}$$

Different RL methods have been proposed to solve the above equations. In some algorithms the agent will first approximate the model of the system in order to calculate the Q-function. The method used in this chapter is of temporal difference type which learns the model of the system under control. The only available information is the reward achieved by each taken action and the next state. The algorithm, called Q-learning, will approximate the Q-function and by the computed function the optimal policy, which maximizes this function, is derived.

3.2 Multi-agent RL

A multi-agent system [43] can be defined as a group of autonomous, interacting entities (agents) [44] sharing a common environment, which they perceive with sensors and upon which they act with actuators [42]. Multi-agent systems can be used in a wide variety of domains including robotic teams, distributed control, resource management, collaborative decision support systems. Well-understood algorithms with good convergence and consistency properties are available for solving the single-agent RL task, both when the agent knows the dynamics of the environment and the reward function (the task model), and when it does not. However, the scalability of algorithms to realistic problem sizes is problematic in single-agent RL, and is one of the great reasons to use multi-agent reinforcement learning (MARL) [12]. In addition to scalability and benefits owing to the distributed nature of the multi-agent solution, such as parallel computation, multiple RL agents may utilize new benefits from sharing experience, e.g., by communication, teaching, or imitation [12]. These properties make RL attractive for multi-agent learning. However, several new challenges arise for RL in multi-agent systems. In multi-agent systems other adapting agents make the environment no longer stationary, violating the Markov property that traditional single agent behavior learning relies on, this nonstationarity properties decrease the convergence properties of most single-agent RL algorithms [46]. Another problem is the difficulty of defining a good learning goal for the multiple RL agents [12]. Only then it will be able to coordinate its behavior with other agents. These challenges make the MARL design and learning difficult in large-scale applications, therefore it uses a special learning algorithm as

below. Using this learning algorithm, the violating the Markov property problem causes from multi-agent structure and other problems will be solved.

Learning Algorithm

The generalization of the Markov decision process to the multi-agent case is as follows:

Suppose a tuple $< X, A_1, \ldots, A_n, p, r_1, \ldots, r_n >$ where n is the number of agents, X is the discrete set of environment states, A_i , $i = 1, \ldots, n$ are the discrete sets of actions available to the agents, yielding the joint action set $A = A_1 \times \cdots \times A_n$, $p: X \times A \times X \to [0,1]$ is the state transition probability function, and $r_i : X \times A \times X \to R, i = 1, \ldots, n$ are the reward functions of the agents.

In the multi-agent case, the state transitions are the result of the joint action of all the agents, $a_k = \left[a_{1,k}^T, \ldots, a_{n,k}^T\right], a_k \in A, a_{i,k} \in A_i$ (T denotes vector transpose). As a result, the rewards $r_{i,k+1}$ and the returns $R_{i,k}$ also depend on the joint action. The policies $h_i : X \times A_i \to [0,1]$ form together the joint policy h. The Q-function of each agent depends on the joint action and is conditioned on the joint policy, $Q_i^h : X \times A \to R$ [33].

4 The Proposed Intelligent Control Framework

In practice, the LFC system is traditionally using a proportional-integral (PI) type controller as shown in Fig. 8. In this section, an intelligent control design algorithm for such a controller using MARL technique is presented. The design objective is to regulate the frequency in power system concerning the integration of wind power units with various load disturbances.

Fig. 9 shows the proposed model for area *i*, including an intelligent controller. The controller is responsible to produce an appropriate control action (ΔP_{ci}) according to the *ACE* signal using RL.

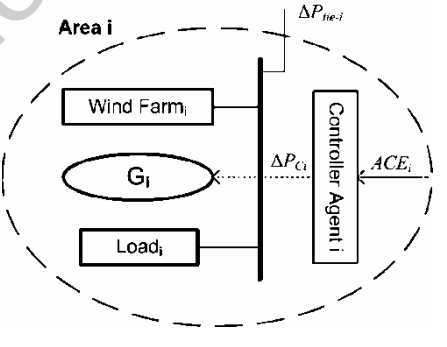

Fig. 9. The proposed model for area *i*

4.1 Controller Agent

The intelligent controller (controller agent) system functions as follows. At each instant (on a discrete time scale k), $k = 1,2,\cdots$ the controller agent observes the current state of the system, x_k, and takes an action, a_k. The state vector consists of some quantities, which are normally available to the controller agent. Here, the average of ACE signal over the time interval $k-1$ to k as the state vector at the instant k is used. For the algorithm presented in this paper, it is assumed that the set of all possible states X, is finite. Therefore the values of various quantities that constitute the state information should be quantized.

The possible actions of the controller agent are the various values of ΔP_c, that can be demanded in the generation level within an LFC interval. ΔP_c is also discretised to some finite number of levels. Now, since both X and A are finite sets, a model for this dynamic system can be specified through a set of probabilities.

Here, an RL algorithm is used for estimating Q^* and the optimal policy. It is similar to the introduced algorithm in [4]. Suppose we have a sequence of samples (x_k, x_{k+1}, a_k, r), $k = 1,2,\cdots$. Each sample is such that x_{k+1} is the (random) state that resulted when action a_k is performed in state x_k and $r_k = g(x_k, x_{k+1}, a_k)$ is the consequent immediate reinforcement. Such a sequence of samples can be obtained either through a simulation model of the system or observing the actual system in operation. This sequence of samples (called training set) can be used to estimate Q^*. Using a specific algorithm. Suppose Q^k is the estimate of Q^* at kth iteration. Let the next sample be (x_k, x_{k+1}, a_k, r), then we obtain Q^{k+1} as:

$$Q^{k+1}(x_k, a_k) = Q^k(x_k, a_k) + \alpha\left[g(x_k, x_{k+1}, a_k) + \gamma \max_{a \in A} Q^k(x_{k+1}, \acute{a}) - Q^k(x_k, a_k)\right] \tag{8}$$

where $0 < \alpha < 1$ is a constant called the step size of learning algorithm.

At each time step (as determined by the sampling time for the LFC action) the state input vector, x, to the LFC is determined, then an action in that state is selected and applied to the model, the model is integrated for a time interval equal to the sampling time of LFC to obtain the state vector $\acute{x}$ at the next time step.

Here, the exploration policy for choosing actions in different states is used. It is based on a Learning automata algorithm called pursuit algorithm [39]. This is a stochastic policy where, for each state x, actions are chosen based on a probability distribution over the action space. Let P_x^k denote the probability distribution over the action set for state vector x at the kth iteration of learning. That is, $P_x^k(a)$ is the probability of choosing action a in state x at iteration k. A uniform probability distribution is considered at $k = 0$, that is

$$P_x^0(a) = \frac{1}{|A|} \quad \forall a \in A \ \forall x \in X \tag{9}$$

At the kth iteration, let the state x_k be equal to x. An action a_k, at random based on $p_x^k(.)$ is chosen. That is, $Prob(a_k = a) = p_x^k(a)$. Using the performed simulation model, the system is gone to the next state x_{k+1} by applying action a in the state x and is integrated for the next time interval. Then, Q^k is updated to Q^{k+1} using (8) and the probabilities is updated as follows, too.

$$P_x^{k+1}(a_g) = P_x^k(a_g) + \beta\left(1 - P_x^k(a_g)\right)$$

$$P_x^{k+1}(a) = P_x^k(a)(1-\beta) \quad \forall a \in A, a \neq a_g \tag{10}$$

$$P_y^{k+1}(a) = P_y^k(a) \quad \forall a \in A, \forall y \in X, y \neq x$$

where $0 < \beta < 1$ is a constant. Thus, at iteration k the probability of choosing the greedy action a_g in state x is slightly increased and the probabilities of choosing all other actions in state x are proportionally decreased.

Learning the Controller

In the present algorithm, the aim is to achieve the well-known LFC objective and to keep the *ACE* within a small band around zero. This choice is motivated by the fact that all the existing LFC implementations use this as main control objective and hence, it will be possible for us to compare the proposed RL approach with the designed linear PI based LFC approaches. As mentioned above, in this formulation, each state vector consists of the average value of *ACE* as state variable. The control action of the LFC is to change the generation set point, ΔP_c. According to the RL algorithms application, usually a finite number of states are assumed. In this direction, state variable and action variable should be discretised to finite levels, too.

The next step is to choose an immediate reinforcement function by defining the function g. The reward matrix initially is full of zero, at each time step we get the average value of *ACE* signal, then according to its discritised values, determine the state of the system, whenever the state is desirable (i.e. $|ACE|$ is less than ε) then reward function $g(x_k, x_{k+1}, a_k)$ is assigned at zero value. When it is undesirable (i.e. $|ACE| > \varepsilon$), then $g(x_k, x_{k+1}, a_k)$ is assigned a value -$|ACE|$ (we penalized all actions which cause to go to an undesirable state with a negative value).

5 Application to the 3-Control Area Test System

To illustrate the effectiveness of the proposed control strategy, and to compare the results with a conventional PI control design, the described 39-bus system (Section 2.2) is considered as a test case study. A block schematic diagram of the model used for simulation studies is shown in Fig. 10 and the proposed multi-agent structure is shown in Fig. 11.

Here, the purpose is essentially to clearly show the various steps in implementation and illustrate the method. After design choices are made, the controller is trained by running the simulation in the learning mode as explained in Section 2.4. After completing the learning phase, the control actions at various states have converged to their optimal values.

The simulation is run as follows: At each LFC instant k, controller agents of each area, average all corresponding ACE signal instances gained every 0.1 seconds. Three average values of ACE signal instances (each related to one area) form the current state vector, x_k, that is obtained according to the quantized states. When all area's state vectors are ready, then the controller agents choose the action signal a_k that consists of three ΔP_c values for three areas (action signal is gained according to the quantized actions and the exploration policy mentioned above) to change the set points of the governors using the values given by a_k.

In the performed simulation studies, the input variable is obtained as follows. As the LFC decision cycle time chosen, three values of ACE are calculated over a decision cycle. The averages of these values for three areas are the state ble $(x^1_{avg1}, x^1_{avg2}, x^1_{avg3})$. Since, we use the multi-agent reinforcement learning process and agents of all areas are learning together, the state vector is also consisted of all state vectors of three areas, the action vector is consisted of all action vectors of three areas as shown in term $< (X_1, X_2, X_3), (A_1, A_2, A_3), p, (r_1, r_2, r_3) >$ or $< X, A, p, r >$.

Here $X_i = x^1_{avgi}$ is the discrete set of each area states, X is the joint state, A_i is the discrete set of each area actions available to the area i, and A is the joint action. In each instant time after averaging of ACE_i for each area (over three instances), depending on the current joint state (X_1, X_2, X_3), the joint action $(\Delta P_{c1}, \Delta P_{c2}, \Delta P_{c3})$ is chosen according to the exploration policy. Consequently, the reward r is also depends on the joint action which whenever the next state (X) is desirable (i.e. all $|ACE_i|$ are less than ε), then reward function r is assigned a zero value. When the next state is undesirable (i.e. $\exists\ ACE_i \mid |ACE_i| > \varepsilon$) then r is assigned average value of -$|ACE_i|$. In this algorithm, since all agents learn together, parallel computation causes to speed up the learning process. Also this reinforcement learning algorithm is more scalable than single-agent RL.

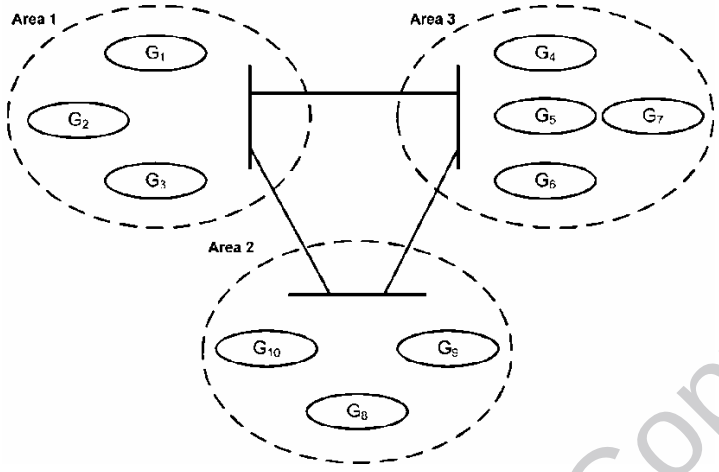

Fig. 10. 3-control area power system

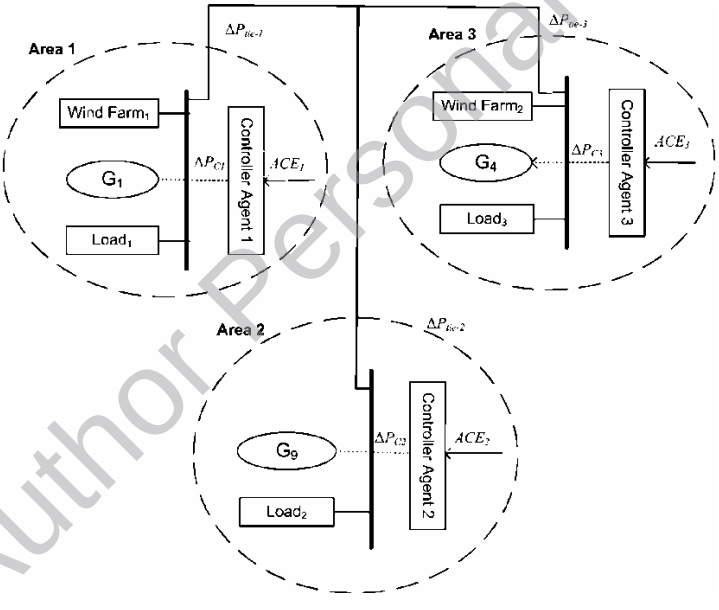

Fig. 11. The proposed multi-agent structure for 3-control area power system

6 Simulation Results

To demonstrate the effectiveness of the proposed control design, some simulations were carried out. In these simulations, the proposed controllers were applied to the model described in Section 2.2. In this section, the performance of the closed-loop

system using the well-tuned conventional PI controllers is compared to the designed MARL controllers for the various possible load disturbances.

As a serious test scenario, the following load disturbances (step increase in demand) are applied to three areas: In Area 1, 3.8% of total area load at bus 8, 4.3% of total area load at bus 3 in Area 2, and 6.4% of total area load at bus 16 in Area 3 have been simultaneously increased in a step form. The frequency deviation (Δf), and area control error (ACE) signals of the closed-loop system are shown in Fig. 12, Fig. 13, and Fig. 14.

As shown in the simulation results, using the proposed method, the area control error and frequency deviation of all areas are properly driven close to zero. Furthermore, regarding that the proposed algorithm is an adaptive algorithm and it is based on the learning methods - in each state it finds the local optimum solution to gain the system objectives (ACE signal near zero) - therefore the intelligent controllers provide smoother control action signals and areas frequency deviation is less than the frequency deviation in the system with PI controllers.

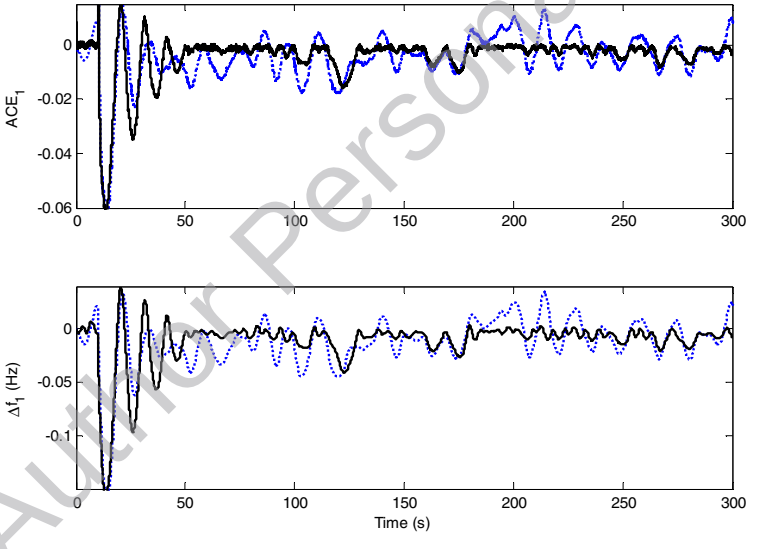

Fig. 12. Area-1 responses; proposed intelligent method (solid), linear PI control (dotted)

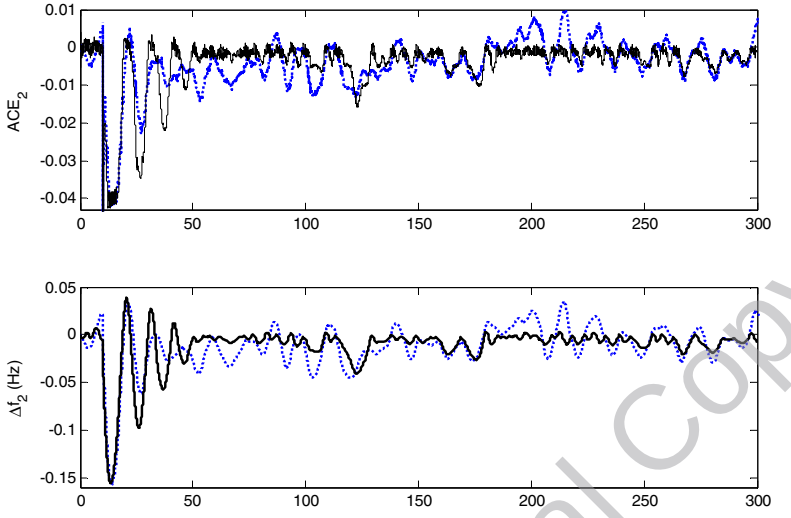

Fig. 13. Area-2 responses; proposed intelligent method (solid), linear PI control (dotted)

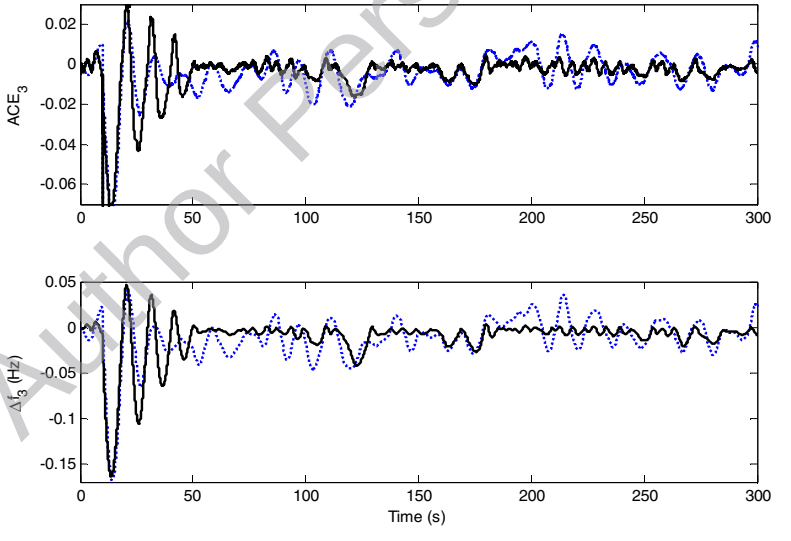

Fig. 14. Area-3 responses; proposed intelligent method (solid), linear PI control (dotted)

7 Summary

This chapter presents an overview of the key issues concerning the integration of WTGs into the power system frequency regulation, that are of most interest today. The most important issues with the recent achievements in this literature are briefly reviewed. The impact of WTGs on frequency control problem is described. An updated LFC model is introduced. Power system frequency response in the presence of WTGs and associated issues is analyzed, and the need for the revising of frequency performance standards is emphasized.

A new method for frequency regulation concerning the integration of wind power units, using MARL has been proposed. The proposed method was applied to a network with the same topology, known as New England 10-generators 39-bus system. The results show that the new algorithm performs well, in comparison of the performance of a PI control design. Two important features of new approach, model independence and flexibility in specifying the control objective; make it very attractive for application in power system operation and control. However, the scalability of MARL to realistic problem sizes is one of the great reasons to use it. In addition to scalability and benefits owing to the distributed nature of the multi-agent solution, such as parallel computation, multiple RL agents may utilize new benefits from sharing experience, e.g., by communication, teaching, or imitation.

References

1. Abbey, C., et al.: Transient Modeling and Comparison of Wind Generator Topologies. In: IPST 2005, p. IPST05 - 131 (2005) (in Canada)
2. Abe, K., Ohba, S., Iwamoto, S.: New load frequency control method suitable for large penetration of wind power generations. In: Power Engineering Society General Meeting (2006)
3. Ahamed, T.P.I.: A neural network based automatic generation controller design through reinforcement learning. International Journal of Emerging Electric Power Systems 6 (2006)
4. Ahamed, T.P.I., Rao, P.S.N., Sastry, P.S.: A reinforcement learning approach to automatic generation control. Electric Power Systems Research 63, 9–26 (2002)
5. Ahamed, T.P.I., Rao, P.S.N., Sastry, P.S.: Reinforcement learning controllers for automatic generation control in power systems having reheat units with GRC and deadband. International journal of power and energy systems 26, 137–146 (2006)
6. Anderson, P.M.: Power System Protection. IEEE/Wiley, New York (1999)
7. Atic, N., Feliachi, A., Rerkpreedapong, D.: CPS1 and CPS2 compliant wedge-shaped model predictive load frequency control. In: Power engineering society general meeting, vol. 1, pp. 855–860. IEEE, Los Alamitos (2004)
8. Banakar, H., Luo, C., Teck Ooi, B.: Impacts of wind power minute-to-minute variations on power system operation. IEEE Transactions on Power Systems 23, 150–160 (2008)

9. Bevrani, H., Hiyama, T.: On load-frequency regulation with time delays: design and real-time implementation. IEEE Transaction on Energy Conversion 24, 292–300 (2009)
10. Bevrani, H., Hiyama, T.: Robust load-frequency regulation: a real-time laboratory experiment. Optimal Control Appl. Methods 28, 419–433 (2007)
11. Bevrani, H.: Robust power system frequency control, 1st edn. Springer, Heidelberg (2009)
12. Busoniu, L., Babuska, R., De Schutter, B.: A comprehensive survey of multi-agent reinforcement learning. IEEE Transaction on Syst., Man., Cyber., Part C: Applications and Reviews 38, 156–172 (2008)
13. Chedid, R.B., Karaki, S.H., El-Chamali, C.: Adaptive fuzzy control for wind-diesel weak power systems. IEEE Transactions on Energy Conversion 15, 71–78 (2000)
14. Demiroren, A., Zeynelgil, H.L., Sengor, N.S.: Automatic generation control for power system with SMES by using neural network controller. Electr. Power Comp System 31, 1–25 (2003)
15. Dokopoulos, P.S., Saramourtsis, A.C., Bakirtzis, A.G.: Prediction and evaluation of the performance of wind-diesel energy systems. IEEE Transactions on Energy Conversion 11, 385–393 (1996)
16. Eftekharnejad, S., Feliachi, A.: Stability enhancement through reinforcement learning: load frequency control case study. Bulk Power System Dynamics and Control VII, 1–8 (2007)
17. Ernst, D., Glavic, M., Wehenkel, L.: Power system stability control: reinforcement learning framework. IEEE Transaction on Power System 19, 427–436 (2004)
18. Gjengedal, T.: System control of large scale wind power by use of automatic generation control (AGC). In: CIGRE/PES, 15–21 (2003)
19. Hall, D.J., Colclaser, R.G.: Transient modeling and simulation of a tubular solid oxide fuel cell. IEEE Transactions on Energy Conversion 14, 749–753 (1999)
20. Hiyama, T., Zuo, D., Funabashi, T.: Multi-agent based automatic generation control of isolated stand alone power system. In: International conference on power system technology (2002)
21. Hiyama, T., Zuo, D., Funabashi, T.: Multi-agent based control and operation of distribution system with dispersed power sources. In: Transmission and Distribution Conference and Exhibition, Asia Pacific. IEEE/PES (2002)
22. Holttinen, H.: Impact of hourly wind power variation on the system operation in the Nordic Countries. Wind Energy 8(2), 197–218 (2005)
23. Horiuchi, N., Kawahito, T., Sizuki, T.: Power control of induction generator by V/F control for wind energy conversion system. Transactions of IEEJ 118-B, 1170–1176 (1998)
24. Karnavas, Y.L., Papadopoulos, D.P.: AGC for autonomous power system using combined intelligent techniques. Electric power systems research 62, 225–239 (2002)
25. Kodama, N., Matsuzaka, T., Inomata, N.: The power variation control of a wind generator by using probabilistic optimal control. Transactions of IEEJ 121-B, 22–30 (2001)
26. Lalor, G., Mullane, A., O'Malley, M.: Frequency control and wind turbine technologies. IEEE Transaction on Power System 20, 1905–1913 (2005)
27. Lalor, G., Ritchie, J., Rourke, S., Flynn, D., O'Malley, M.J.: Dynamic frequency control with increasing wind generation. In: Power Engineering Society General Meeting (2004)
28. Lalor, G., et al.: Frequency control and wind turbine technologies. IEEE Transaction on Power System 20, 1905–1913 (2005)

29. Lindgren, E., Söder, L.: Minimizing regulation costs in multi-area systems with uncertain wind power forecasts. Wind Energy-Wiley Inter-science 11, 97–108 (2007)
30. Lukas, M.D., Lee, K.Y., Ghezel-Ayagh, H.: Development of a stack simulation model for control study on direct reforming molten carbonate fuel cell power plant. IEEE Transactions on Energy Conversion 14, 1651–1657 (1999)
31. Luo Far, C., Banakar, H.G., Pin-Kwan Keung, H., Ooi, B.T.: Estimation of Wind Penetration as Limited by Frequency Deviation. In: Power Engineering Society General Meeting (2006)
32. Morren, J., de Haan, S.W.H., Kling, W.L., Ferreira, J.A.: Primary power/frequency control with wind turbines and fuel cells. In: Power Engineering Society General Meeting (2006)
33. Morren, J., de Haan, S.W.H., Kling, W.L., Ferreira, J.A.: Wind turbines emulating inertia and supporting primary frequency control. IEEE Transactions on Power System 21, 433–434 (2006)
34. Mullane, A.P.: Advanced control of wind energy conversion systems. Ph.D. dissertation, Nat. University of Ireland, Univ. College Cork, Cork, Ireland (2004)
35. Mullane, A., O'Malley, M.: The inertial-response of induction-machine based wind-turbines. IEEE Transaction on Power System 20, 1496–1503 (2005)
36. Sathyajith, M.: Wind Energy Fundamentals, Resource Analysis and Economics, 1st edn., pp. 112–114. Springer, Heidelberg (2006)
37. Senjyu, T., Hayashi, D., Urasaki, N., Funabashi, T.: Oscillation frequency control based on H∞ controller for a small power system using renewable energy facilities in isolated island. In: Power Engineering Society General Meeting (2006)
38. Sutton, R.S., Barto, A.G.: Reinforcement learning: an introduction. MIT Press, Cambridge (1998)
39. Thathachar, M.A.L., Harita, B.R.: An estimator algorithm for learning automata with changing number of actions. International Journal of General Systems 14, 169–184 (1988)
40. The United Nations Framework Convention on Climate Change, The Kyoto Protocol (1997), http://unfccc.int/resource/docs/convkp/kpeng.pdf (accessed June 28, 2008)
41. Vittal, E., et al.: Varying Penetration Ratios of Wind Turbine Technologies for Voltage and Frequency Stability. In: Power and Engineering Society General Meeting, vol. 20, pp. 1–6 (2008)
42. Vlassis, N.: A concise introduction to multi-agent systems and distributed AI. Fac. Sci. Univ. Amsterdam, Amsterdam, The Netherlands, Tech. Rep. (2003)
43. Weiss, G. (ed.): Multi-agent systems: a modern approach to distributed artificial intelligence. MIT Press, Cambridge (1999)
44. Wooldridge, M., Weiss, G. (eds.): Intelligent agents, in multi-agent systems, pp. 3–51. MIT Press, Cambridge (1999)
45. Du, X., Li, P.: Fuzzy logic control optimal realization using GA for multi-area AGC systems. International Journal of Information Technology 12, 63–72 (2006)
46. Gu, Y.: Multi-agent reinforcement learning for multi-robot systems: a survey. Technical Report, CSM-404 (2004)

Appendix

39-Bus Test System Parameters

Generators

All generators are conventional thermal type and are treated as the sixth order machine model. Parameters for two axis model of the synchronous machine are shown in Table 1. For each generator, all values are given in per unit on its base values.

PSS

The power system stabilizer (PSS) is modeled as shown in Fig. 15. All generators are equipped with identical PSSs. PSS parameters are shown in Table 2.

Table 1. Generator parameters

Unit no.	H [s]	X_d'' [pu]	X_d' [pu]	X_d [pu]	X_q'' [pu]	X_q' [pu]	X_q [pu]	X_l [pu]	R_a [pu]	T_{do}'' [s]	T_{do}' [s]	T_{qo}'' [s]	T_{qo}' [s]	T_d'' [s]	T_d' [s]	T_q'' [s]	T_q' [s]	P_n [MW]	V_n [kv]
1	4.768	0.134	0.174	1.220	0.134	0.250	1.160	0.078	0.004	0.033	8.970	0.070	0.500	0.023	1.280	0.023	0.640	120	15.5
2	4.768	0.134	0.174	1.220	0.134	0.250	1.160	0.078	0.004	0.033	8.970	0.070	0.500	0.023	1.280	0.023	0.640	120	15.5
3	6.1867	0.130	0.185	1.050	0.130	0.850	1.240	0.070	0.0031	0.038	6.100	0.070	0.500	---	---	0.023	0.640	75	13.8
4	6.1867	0.130	0.185	1.050	0.130	0.360	0.980	0.070	0.0031	0.038	6.100	0.070	0.500	---	---	0.023	0.640	73.2	13.8
5	6.1867	0.130	0.185	1.050	0.130	0.850	1.240	0.070	0.0031	0.038	6.100	0.070	0.500	---	0.882	0.023	0.640	64	13.8
6	6.1867	0.130	0.185	1.050	0.130	0.360	0.980	0.070	0.0031	0.038	6.100	0.070	0.500	---	---	0.023	0.640	75	13.8
7	6.1867	0.130	0.185	1.050	0.130	0.850	1.240	0.070	0.0031	0.038	6.100	0.070	0.500	---	0.882	0.023	0.640	66	13.8
8	6.1867	0.130	0.185	1.050	0.130	0.850	1.240	0.070	0.0031	0.038	6.100	0.070	0.500	---	0.882	0.023	0.640	64	13.8
9	4.768	0.134	0.174	1.220	0.134	0.250	1.160	0.078	0.004	0.033	8.970	0.070	0.500	0.023	1.280	0.023	0.640	120	15.5
10	6.1867	0.130	0.185	1.050	0.130	0.850	1.240	0.070	0.0031	0.038	6.100	0.070	0.500	---	0.882	0.023	0.640	64	13.8

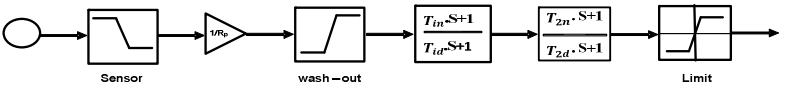

Fig. 15. PSS block diagram

Table 2. PSS parameters

Senor Time constant	K	Wash-out Time constant	T_{1n}	T_{1d}	T_{2n}	T_{1d}	V_{smin}	V_{sma_x}
0.015	3.125	1	0.060	1	0	0	-0.15	0.15

Governor

The turbine-governors in the test system are modeled as shown in Fig.16, and the related parameters are shown in Table 3.

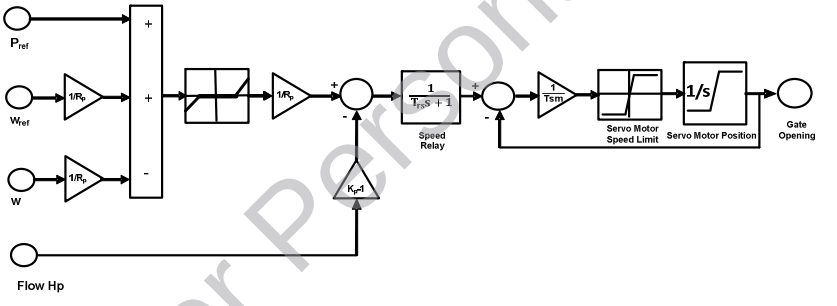

Fig. 16. Turbine-governor block diagram

Table 3. Governor Parameters

k_p	R_p[pu]	DZ[pu]	T_{sr}[s]	T_{sm}[s]	V_{gmin}	V_{gmax}	g_{min}[pu]	g_{max}[pu]
1	0.05	0	0.001	0.15	-0.1	0.1	0	1

Loads

Loads are treated as constant impedance loads and shown in Table 4. The active and reactive powers absorbed by the loads are proportional to the square of the system voltage.

Table 4. Load values

Bus	P[MW]	Q[MVar]
1	0	0
2	0	0
3	21.47	0.24
4	50	18.4
5	0	0
6	0	0
7	23.38	8.4
8	52.2	17.66
9	0	0
10	0	0
11	0	0
12	0.75	8.8
13	0	0
14	0	0
15	32	15.3
16	32.9	3.23
17	0	0
18	10.533	2
19	0	0
20	62.8	10.3
21	27.4	11.5
22	0	0
23	24.75	8.46
24	15.43	9.22
25	11.2	2.36
26	13.9	1.7
27	18.73	5.03
28	20.6	2.76
29	28.35	2.69
31	0.92	0.46
39	138	31.52

Line/Transformers

The line parameters of the test system are shown in the Table 5. For each transformer, all values are given in per unit (on its MVA base), and are given in Table 6.

Table 5. Line parameters

Line Data					
From bus	To bus	R [ohm/km]	L [H/km]	C [F/km]	Length
1	2	35e-4	1.0902 e-4	18.534 e-8	10
1	39	1e-3	6.6315 e-5	19.894 e-8	10
2	3	3.25e-3	10.0135 e-5	17.056 e-8	4
2	25	28e-3	9.1248 e-5	15.4912 e-8	2.5
3	4	2.6e-3	11.3e-5	11.7456 e-8	5
3	18	2.75 e-3	8.8197 e-5	14.178 e-8	4
4	5	26.667 e-4	11.3176 e-5	11.866 e-8	3
4	14	26.667 e-4	11.406 e-5	12.2197 e-8	3
5	6	40 e-4	13.7934 e-5	23.024 e-8	0.5
5	8	26.667 e-4	9.903 e-5	13.0506 e-8	3
6	7	24 e-4	9.7616 e-5	11.9896 e-8	2.5
6	11	28 e-4	8.7004 e-5	14.7376 e-8	2.5
7	8	26.667 e-4	8.1346 e-5	13.7933 e-8	1.5
8	9	2.5555 e-3	10.6988 e-5	11.2111 e-8	9
9	39	1 e-3	6.6315 e-5	31.831 e-8	10
10	11	40 e-4	11.406 e-5	19.337 e-8	1
10	13	40 e-4	11.406 e-5	19.337 e-8	1
13	14	30 e-4	8.9303 e-5	15.2347 e-8	3
14	15	2.7692 e-3	8.8555 e-5	14.9361 e-8	6.5
15	16	30 e-4	8.3113 e-5	15.1197 e-8	3
16	17	28 e-4	9.4432 e-5	14.2392 e-8	2.5
16	19	3.2 e-3	10.345 e-5	16.1278 e-8	5
16	21	20 e-4	8.9525 e-5	16.897 e-8	4
16	24	20 e-4	10.4333 e-5	12.0253 e-8	1.5
17	18	28 e-4	8.7004 e-5	13.9952 e-8	2.5
17	27	2.6 e-3	9.178 e-5	17.0614 e-8	5
21	22	17.777 e-4	8.2524 e-5	15.1198 e-8	4.5
22	23	20 e-4	8.4883 e-5	16.3223 e-8	3
23	24	2.75 e-3	11.605 e-5	11.9697 e-8	8
25	26	3.5555 e-3	9.5198 e-5	15.12 e-8	9
26	27	3.5 e-3	9.7482 e-5	15.889 e-8	4
26	28	3.5833 e-3	10.4775 e-5	17.2458 e-8	12
26	29	3.3529 e-3	9.7523 e-5	16.0558 e-8	17
28	29	3.5 e-3	10.0135 e-5	16.5122 e-8	4

Table 6. Transformer parameters

From bus	To bus	R [ohm/km]	L [H/km]	C [F/km]	S_n [MVar]	Tap Data	
						Magnitude [pu]	Angle [degree]
12	11	0.08e-3	2.175 e-3	0	50	1	0
12	13	0.08e-3	2.175 e-3	0	50	1	0
6	31	0	6.250 e-3	0	250	1	0
10	32	0	5.000 e-3	0	250	1	0
19	33	0.175 e-3	3.550 e-3	0	250	1	0
20	34	0.225 e-3	4.500 e-3	0	250	1	0
22	35	0	3.575 e-3	0	250	1	0
23	36	0.125 e-3	6.800 e-3	0	250	1	0
25	37	0.150 e-3	5.800 e-3	0	250	1	0
2	30	0	4.525 e-3	0	250	1	0
29	38	0.2 e-3	3.900 e-3	0	250	1	0
19	20	0.175 e-3	3.450 e-3	0	250	1	0